FBMIS Volume 1, 2006, 48-69 ISSN 1740-5955
http://www.fbmis.info/6_1_DeanC_1

IMPROVING VISUALISATION OF MATURE, HIGH-CARBON-SEQUESTERING FORESTS

CHRISTOPHER DEAN[1] and STEPHEN ROXBURGH[2]

[1]Forest Products Commission, 1/117 Great Eastern Highway, Rivervale, WA 6103, Australia.
christopher.dean@fpc.wa.gov.au
[2]School of Biological, Earth and Environmental Sciences, The University of New South Wales & Bushfire Cooperative Research Centre, Ensis, PO Box E4008, Kingston, ACT 2604, Australia.
stephen.roxburgh@ensisjv.com

(Submitted, 16th Dec. 2005; Accepted, 14 Nov. 2006; Published, 6 Dec. 2006)

ABSTRACT

This work presents results from the landscape-level carbon-sequestration-forecasting model CAR4D, by way of visualisation. We start by comparing the standing sequestered carbon, calculated by different means, for three similar oldgrowth (silviculturally overmature) forests of relatively high biomass. We then proceed to long-term steady states under different management options, landscape-level differences, fire scenarios, fly-throughs and 3D animation of growth.

Carbon sequestered in live biomass of the eucalypts/total-forest were: *E. regnans* (Tasmania):—600/850 t-C/ha; *E. obliqua* (Tasmania)—732/760 t-C/ha; and *E. regnans* (Victoria, Van Pelt *et al*., 2004):—914/953 t-C/ha. The differences in these values of sequestration for these sites were not necessarily matched to individual trees' yields based on site index but were more related to stand-level effects: a) the rate of self thinning, and b) height growth due to competition, and possibly higher than expected error margins in allometrics. This unexpected result indicated a need for models that are more comprehensive at various levels.

In this study, the appearance of mature trees on hilly terrain varies greatly, depending on the direction and amount of the spur development in the buttress and on local topography. Measurements were undertaken to detect any connection between spur development and slope direction. The cross-sectional shape of several mature trunks at 1.3 metres height on slopes of up to 25° was obtained. No definitive directional preference for spur development was found, but instead a diversity of buttress shapes and micro-habitats on steep slopes.

Taper equations are the most scientifically representative method for rendering the trunks of mathematically derived forests. Five taper equations were tested on various sizes of *Eucalyptus regnans*. Two new equations allowed better fits for individual trees. The overall best fit equation was based on first principles of tree growth plus an extra parameter for buttress shape—totalling six parameters. That equation was combined with realistic cross-sections to calculate whole-trunk 3D VRML models as a function of DBH. A complex adjustment to trunk shape was included for uneven, sloping ground. Animation of trunk growth was created by general expansion of the perimeter of cross-sections combined with preferential expansion corresponding to spurs. For more mature trees the preferential expansion was reduced, corresponding to achievement of structural stability. Tree trunks and animations were rendered in VRML format. The result allowed within-stand models, including growth, to be rendered and visualised by still frames or by fly-throughs.

Keywords: sequestration, eucalyptus regnans, taper, visualisation, buttress, animation.

1 INTRODUCTION

The carbon sequestration and forecasting program, CAR4D, was first described at the workshop 'Reality, Modelling and Parameter Estimation - the Forestry Scenario' held in Sesimbra, Portugal, in 2002. Details of field methodology and much of the allometrics in CAR4D are given in a series of papers: Dean (2003), Dean *et al.* (2003) and Dean *et al.* (2004). The model has since been enhanced to cater for the impact of fire, updated allometrics, and 3D animation. In this paper we show: visualisation of the internal structure of CAR4D, examples of analyses and results using CAR4D via different pictorial styles (different ways of visualisation), and show details of development of 3D animation for views from within the forest (known as "within-stand").

CAR4D provides a carbon sequestration forecast for *Eucalyptus regnans* forests or plantations across varying environments, ages, fire events and management regimes. The name is an abbreviation for following the passage of carbon through the three Cartesian dimensions plus time. The modelling in CAR4D (as referred to above) and the results from CAR4D are unique in that they:

(a) cater for ages up to 450 yrs (including senescence), which is well beyond the usual maximum of 100 yrs in previous *E. regnans* growth models, and they cater for DBH sizes up to the maximum recorded for *E. regnans* (~11m, Ashton, 1975);
(b) include the sequestration legacy acquired over many growth cycles (up to a steady state) for different micro-environments across the landscape; and
(c) the allometrics were comprehensively devised from a wide range of published, unpublished and contributed data sources (e.g. diameter distributions for different aged stands from David Ashton (Melbourne University, 2002, personal communication) and management area (coupe) logging records held by Forestry Tasmania (Hobart, 2002, personal communication)), and from data collected in our own fieldwork.

Although the model is currently parameterised only for *E. regnans* the approaches used and the results obtained are applicable to a wider range of species that are similarly significant to both resource extraction, carbon sequestration and conservation activities. Briefly, CAR4D caters for a range of carbon pools such as stem, leaves, roots and branches, soil carbon, coarse woody debris (CWD), fine litter fall, and the wood products: pulpwood and sawlog. Output from the model can be in various forms:

(a) tabular as a function of time for a unit area (in tonnes of carbon per hectare),
(b) tabular as a function of time for a bounded landscape (e.g. in Megatonnes of carbon per catchment),
(c) in GIS grid format for a bounded landscape, with separate grids for different years in the forecast,
(d) as a rudimentary stand-level VRML format (virtual reality modelling language, version 2.0)—a 3D option currently under development.

The 3D VRML format could be useful in studying carbon dynamics, e.g. for comparing different models, or for forest management or ecological studies. Applications for forest trees in computer graphics are varied, e.g.: children's movies (e.g. Barnard, 2000), influencing opinion on resource extraction (e.g. Bishop *et al*. 2003), harvesting machine simulators (CMLabs, circa 2003), immersive virtual reality (Gigliotti, 2002), games (e.g. Szijártó & Koloszár, 2003), and ecological studies (e.g. Dzierzon *et al*. 2003).

Models of carbon sequestration in forest or woodland ecosystems require formulation of growth over life-cycles of the trees, including silviculturally overmature (oldgrowth) trees, and they are a focal point in this work. The present work on within-stand visualisation was founded on allometrics and observations from fieldwork and it has potential for any of the above mentioned applications.

In forest harvesting there is also the potential to reduce environmental impacts and timber wastage on more difficult terrain by simulating mechanical effects and engineering technology with the use of virtual reality (VR). Ship-handling simulators, which rely on VR, are used to teach pilots skills in the manoeuvring of large commercial vessels and include such mechanical effects as hydrodynamics and accurate rebounds from ship-ship and ship-pier collisions. The same concepts could be applied to forestry where there are limited options once a manoeuvre has taken a wrong turn and where both personal safety and environmental costs can be high. For example, in coupe WE008E, Tasmania (a typical "cable logging" coupe and a fieldwork location for the present study) where working slopes were on average from 20 to 25º (but up to 50º in places) some of the more immediate environmental impacts included mixing of surface soil, bed rock, logging debris, and harvestable timber. Also a

ISSN 1740-5955

logger received broken legs when a cable snapped; and timber wastage occurred due to unexpected snagging during cable pulling (subsequently the cables were cut) and in localities where manual chain sawing was abnormally dangerous large trees were dynamited, resulting in a loss of merchantable timber. Technology and skills adapted to such conditions, with the help of VR, could make field operations safer and less wasteful.

At the landscape-level the usual renditions of carbon cycle models are animated maps or 3D animated column graphs. Modelling of forest growth and carbon sequestration under different growth and management scenarios is currently well studied (e.g. Knauft, 2004, Ervin & Hasbrouck, 2001) but visualisation of the within-stand processes is quite rare and poorly advanced. Visual portrayal of the growth and senescence processes would allow differences between models, and between their results, to be better appreciated. However, the process of choosing which carbon cycle model is best suited to one's data or forecast scenario would be facilitated by biometrically accurate 3D visualisation of the models' flows and stocks from within the forest stand. Also, the 3D data used for such renditions, would allow calculation of the light filtering through the canopy and available for photosynthesis. The graphics presented here are a first step in that direction for mature forests.

Views from within oldgrowth stands are fundamentally different to those for younger stands: (i) the branches and leaves of the canopy species are not obvious when traversing the forest floor; and (ii) the trunks may be an order of magnitude wider at the base than at mid height—up to several metres wide at the base. Such trunks can cover ground containing significant changes in direction and slope, and the points of contact with the ground may have obviously different elevations. The intricacies involved in ascertaining biometrics of such trees suggest that existing stem taper equations do not account for trees on slopes because: (i) taper will appear less severe on slopes due to a systematic error in the standard forestry measurement method; the base level is taken on the upslope side of the tree, higher up than where the original seed germinated, and (ii) taper equations do not reveal the shape of the tree below the base level. The present work provides a first step in producing a 3D rendition of the carbon cycle modelling processes: i.e. renditions of oldgrowth trunks on uneven ground.

2 VISUALISATION AND CAR4D

2.1 Input and processing. The flow chart for CAR4D is shown in Figure 1. The input to CAR4D

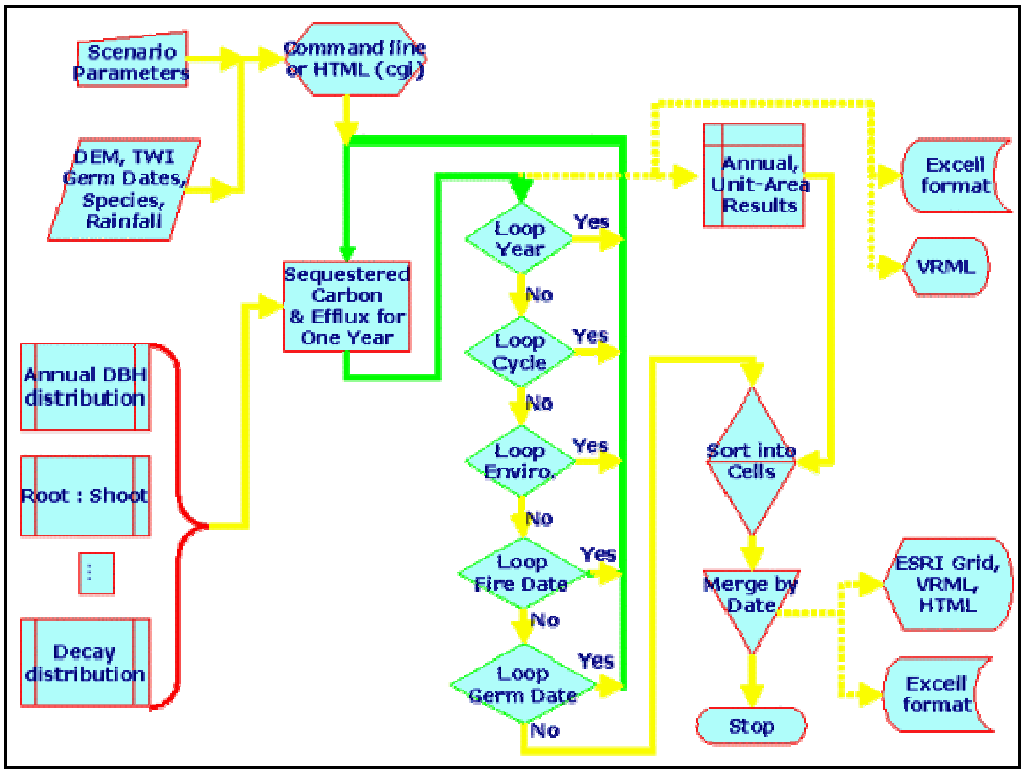

Figure 1. Flow diagram for CAR4D.

is in two main forms: (i) parameters for different scenarios (including management) and (ii) GIS grids (in ESRI ASCII grid format) of environmental conditions (DEM, topographic wetness and summer rainfall), stand germination dates (including uneven-aged stands) and species distribution. The core is the calculation of the carbon that is present, per hectare, for any one year and the efflux for that year. This makes use of a series of preset functions, many of which were given in Dean *et al*. (2003) and Dean *et al*. (2004). Some of the factors parameterised include DBH probability distribution per unit hectare, root:shoot ratios for different ages, canopy senescence and coarse woody debris (CWD) decay.

The core of CAR4D is centred within concentric loops of age, generation, environment, fire date and germination date. One set of output data contains the annual per hectare results for the average environment. A final set of output data contains the landscape level sequestration forecast as a function of date, and this can be in GIS ASCII grid format. The first eleven growth cycles are calculated then discarded, as they are used only to stabilise a dynamic, steady state for the long-term soil carbon pool (and to a lesser extent the CWD pools) for each environmental category.

CAR4D is designed to be cross-platform (namely UNIX and MS-Windows): it is coded in C++ and the suite of UNIX-simulation freeware from Cygwin was used for its compilation and execution on MS-Windows. The animation controls are coded in Javascript and VRML.

2.2 Point-in-time, unit area calculation—comparison of model output with other methods. This section gives an example of the simplest type of calculation using CAR4D—standing biomass per unit area for a particular forest stand—and we compare that with calculations by other methods and researchers for similar forests. From external measurements of tree size the carbon sequestered in the above-ground, live biomass of a *Eucalyptus regnans* forest has previously been described as the highest for any forest in Australia and only surpassed by some sites in North America (Van Pelt *et al*., 2004). We compared that previous measurement of *E. regnans* with sequestration calculated for two similar forests and the results are shown in Table 1 (examples of each are shown in Figure 2).

Species	Site	Age (yrs)	Stand Density (trees/ha)	Mean DBH (m)	Eucalypt Biomass (t/ha)	Eucalypt + Understorey Biomass (t/ha)
E. regnans	SX004C	321	32.3	2.74	1,200	1,700
E. obliqua	WR005D	450	37.4	2.25	1,465	1,510
E. regnans	WaCr	292	51	2.05	1,828	1,906

Table 1. Biomass for three different forests: SX004C (Styx Valley, Tasmania), WR005D (WarraLTER, Tasmania), and WaCr (Wallaby Creek, Victoria).

The three forests have unique characteristics. The Styx Valley (containing SX004C) is (presently) renown for tall trees (Kostoglou, 2000) and the measurements were taken amongst an understorey of myrtle (with DBHs over 2 m) and sassafras with some celery top (Figure 2.a), which were indicative of a high site index (Mick Brown, Forestry Tasmania, Hobart, 2003, personal communication). The WR005D site (Figure 2.b) was considered to be of low site index judging from the understorey species present and the southerly aspect (Leigh Edwards, Forestry Tasmania, Hobart, 2004, personal communication; Kathryn Allen, dendrochronologist, Hobart, 2003, personal communication). The WaCr site (like that in Figure 2.c) was also considered to be a poorer site judging from the understorey species present (Ashton, 1993). The biomasses for the three forests were calculated by three different means:

(a) WR005D: measurements of DBH and stand density were taken; then biomass calculated from allometrics derived by weighing tree components (Keith *et al*., 2000);
(b) WaCr: volumes of the timber were made by comprehensive arboricultural measurements (Van Pelt *et al*., 2004) and root biomass was added using allometrics (Dean *et al*., 2003); and
(c) SX004C: calculated using DBH and stand density data from the site and allometrics in CAR4D (Dean *et al*., 2003).

The results were not those expected because the eucalypt biomass for the supposedly poorer sites is higher than for the higher site index location (e.g. Van Pelt *et al*., 2004, state that the estimated wood volume for WaCr is the highest recorded for Australia). However, due to the vigorous rainforest type undestorey in the SX004C the total biomass for that forest does exceed that of WR005D.

There are several plausible reasons for the poorer sites having higher eucalypt biomass:

(a) the eucalypt stand density in WaCr is high, even for a poor site, 70% higher than normal (*viz* calculated stand density at 292 yrs for *E. regnans* is 30, Dean *et al*., 2003). The stand density for the WR005D is about 100% higher than normal (cf. Gilbert, 1958);

ISSN 1740-5955

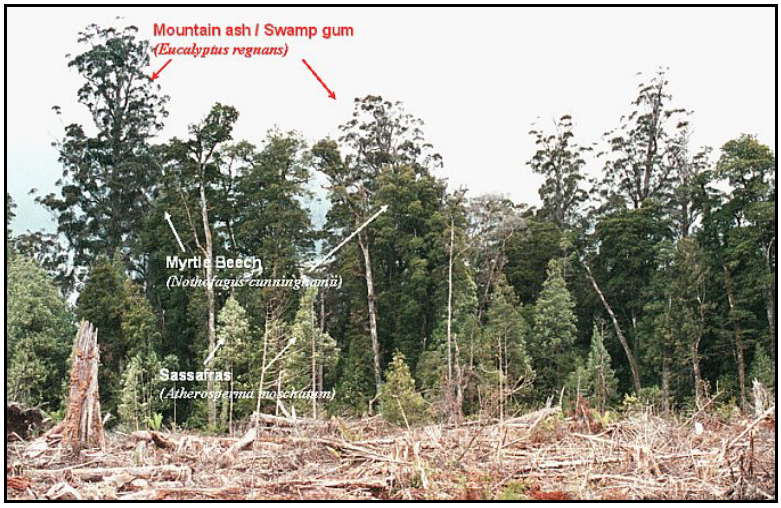

(a)

(b)

(c)

Figure 2. Mature eucalyptus forests of different ages with understoreys of greatly different biomass. (a) Maturing rainforest species in a 320 year old stand of *E. regnans* good quality soil in coupe SX004C in the Styx valley of Tasmania with an understorey of myrtle beech, sassafras and some celery-top pine. (b) A stand of principally *E. obliqua* similar to that in coupe WR005D with a rainforest understory of celery-top pine, blackwood and leatherwood. (c) Scrubby understorey species in a 200 year old *E. regnans* stand possibly on poor soil and subject to heavy snowfall damage or relatively frequent understorey fires, in the Central Highlands of Victoria, typical of that in the O'Shannessy catchment and Wallaby Creek.

(b) CAR4D is known to be conservative with respect to stand biomass for the oldgrowth stage and it is possible that both the calculated eucalypt and understorey biomasses for SX004C were underestimated (as described in Dean *et al*., 2003);
(c) internal stem decay (senescence) was not taken into account when converting the volumes of WaCr to biomass by Van Pelt *et al*. 2004 (however they were for WR005D and SX004C, by the present authors);
(d) the error margins of the estimates have not been considered and it is possible that the three estimates are not significantly different.
(e) although a poorer site has low site index (i.e. shorter trees at age 50 yrs) in some circumstances the canopy may continue to grow vertically if undisturbed (i.e. subject to premature senescence) and if competition is still prevalent, i.e. the potential height may be independent of the site index—indeed the WaCr forest was described by Van Pelt *et al*., (2003) as being one of the world's tallest, and stem volumes were an average 22% higher than those calculated from DBH alone, using CAR4D and heights from Galbraith (1937). In CAR4D the potential individual tree volumes can be decoupled from the effects of site index (leaving site index to affect stand growth rate only) but in CAR4D individual trees on low site index sites can not achieve volumes greater than trees on high site index sites. Consequently CAR4D could presently be used to model a site such as WR005D but not WaCR, i.e. not unless it was modified to allow one site index which affected growth rate and a second, independent site index which affected potential individual-tree volume.

These results suggest that carbon sequestration models need to cater for more variability observed in the environment, to make them more comprehensive models in terms of site-index-dependent growth calculations, carbon sequestration forecasting, and in accompanying visualisation.

2.2 Unit-area output. As an example of the unit-area output consider the scenario where a 321 year old *E. regnans* forest is logged for pulpwood and sawlog, followed a by the standard high-intensity burn, reforestation and 80-year harvesting cycles for sawlog (Figure 3.a): the total carbon (including wood products, CWD, stem, soil etc.) gradually drops with successive harvesting cycles down to a steady state with a cycle-long average of about 400 t-C/ha. But if the forest is not logged but undergoes natural regeneration then the long-term average sequestered carbon is about 1,200 t-C/ha. (The partitioning and longevity of the different wood products was determined from commercial forestry records and published reports, as described in Dean *et al*. 2003. and caters for ages from the younger plantation-like managed stands to oldgrowth stands.)

The reason for the relatively large, long-term drop upon repeated felling is that the *E. regnans* only grow to two thirds of their potential: there is a lot of CWD debris created and there are frequent, intense fires. If the diesel fuel used by logging equipment were included (as in the carbon analysis of Liski *et al*., 2001) and that used in transport then the efflux would be greater and hence so would the drop in long-term average sequestration. For a harvest cycle of length 40 yrs the long-term average is lower (~ 200 t-C/ha for the total carbon) than for a harvest cycle of length 80 yrs.

We conclude from these results that there is a level, long-term steady-state amount of sequestered carbon and that there is not a continued increase with successive cycles due to sequestration in wood products, as was suggested in Grierson *et al*., (1993). When the long-term (e.g. greater than five harvesting cycles) steady states of a range of harvest-cycle lengths were graphed, it was evident that the maximum sequestration in wood products occurs when the cycle length is 50 yrs. The duration of 50 yrs is the same duration as for maximum average annual stem volume increment and for the minimal water output from the *E. regnans* stand (Vertessy *et al*., 2001). Also from the long-term averages it was noticed that the maximum amount sequestered in wood products is doubled if the half-life of the wood products (time taken since harvesting for half the harvested mass to decay) is doubled. (In Figure 3.b the effect of doubling the half-life of the sawlog pool from 20 yrs to 40 yrs is shown as the long-dashed lines, and the effect of halving the understorey biomass is shown as short-dashed lines.) The carbon sequestered in wood products is only a significant portion of the total when the cycle length is less than about 80 yrs. Consequently doubling the half-life of wood products is also only significant for such cycle lengths. However it was evident that the maximum in the total sequestration (including soil carbon and wood products) occurs when the harvest cycle length more closely matches the stand longevity found in nature without frequent disturbance:- somewhere around 400 yrs (depending on the particular genetic stock and environmental conditions).

ISSN 1740-5955

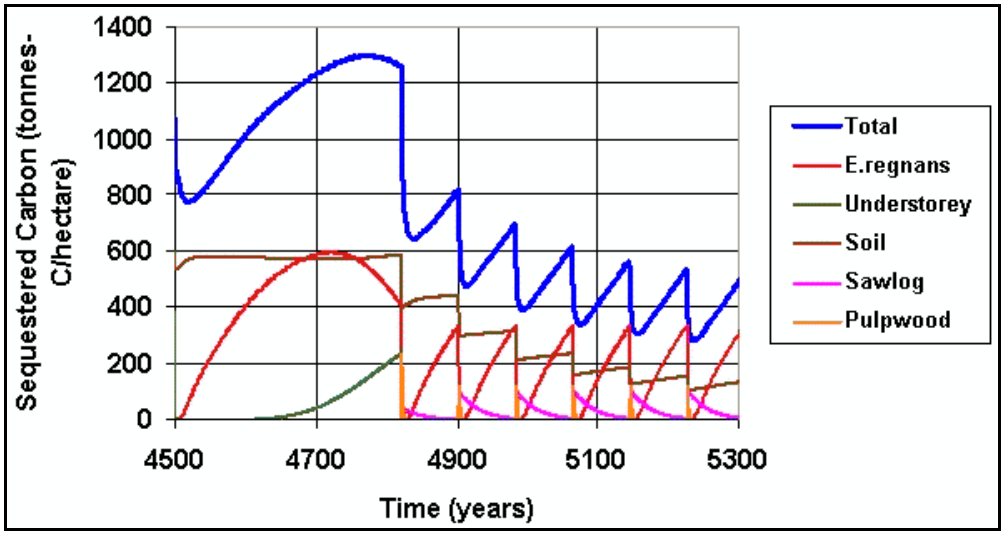

(a)

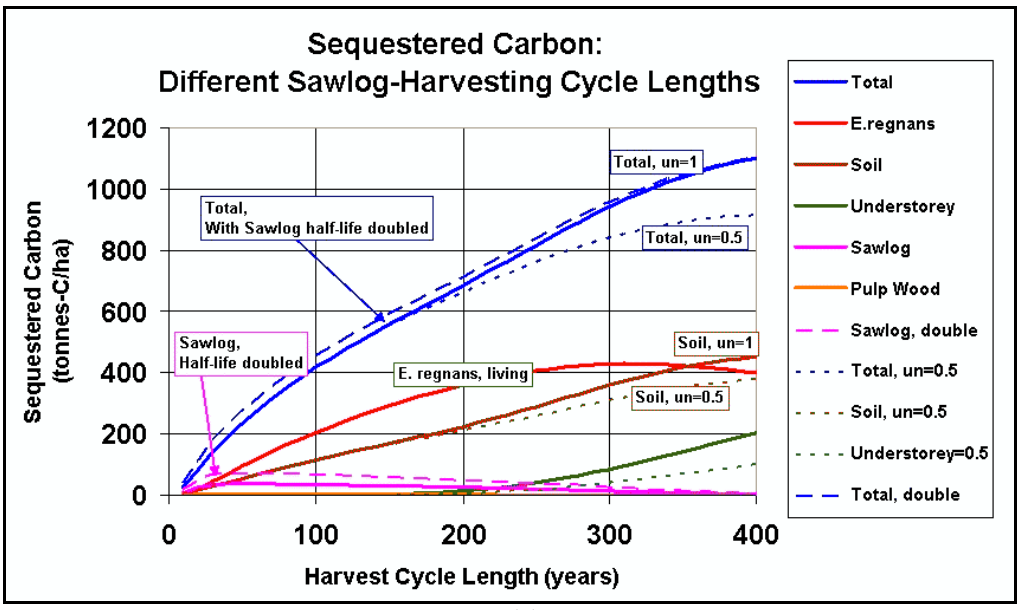

(b)

Figure 3. (a) Sequestered carbon in some of the major pools as a function of time for logging oldgrowth mainly for pulpwood and sawlog followed by an intense burn then reforestation and successive harvest cycles of length 80 yrs. The total carbon drops to steady state, long-term average. (b) The effect of different harvest cycle lengths on some of the major carbon pools. The total sequestered carbon increases with increasing cycle length with a plateau above a cycle length of 400 yrs. The wood products pool has a maximum when the harvest cycle length is about 50 yrs.

2.3 Landscape-level calculations. Spatial variability of the environment is implemented in CAR4D via adjustments to growth and self-thinning as a function of topographic wetness and summer rainfall Dean *et al*. (2004). Stand height has also been stated as being related to many other variables such as genetics, soil depth, latitude etc (e.g. Galbraith, 1937; Cochrane, 1969) but no mathematical relationships were provided and so these factors were not modelled. Higher site-indices mean both increased growth rate (which affects characteristics such as stand density and annual volume increment) and possibly also higher potential, e.g. maximum stem height and different understorey species.

There is uncertainty in carbon sequestration forecasts because of uncertainty in different parameters related to such things as the senescence of the mature *E. regnans*, the amount of understorey, the mean site index for an assessment area, and the influence of competition between mature trees—a choice of different parameters produces a peak of sequestration at different times and of different magnitudes.

There is a lack of information on the frequency of fires that burnt the parent stands before those in existence today. Some future fire frequency scenarios were generated and are shown in Figure 4. Due to the long half-life of soil carbon historical fires make a difference to the present soil carbon legacy—there is a greater separation between the different scenarios if the previous fires were less frequent because the different parameters have a longer period over which to have an effect, before the next fire. For example, considering the two scenarios where (a) there is competition between neighbouring oldgrowth trees, and (b) where the competition is greatly reduced once the trees are over about 200 years of age. In the latter case the stand density doesn't decrease as much and consequently it has larger standing stock of *E. regnans*, a higher carbon sequestration and in turn, eventually more soil carbon owing to senescence.

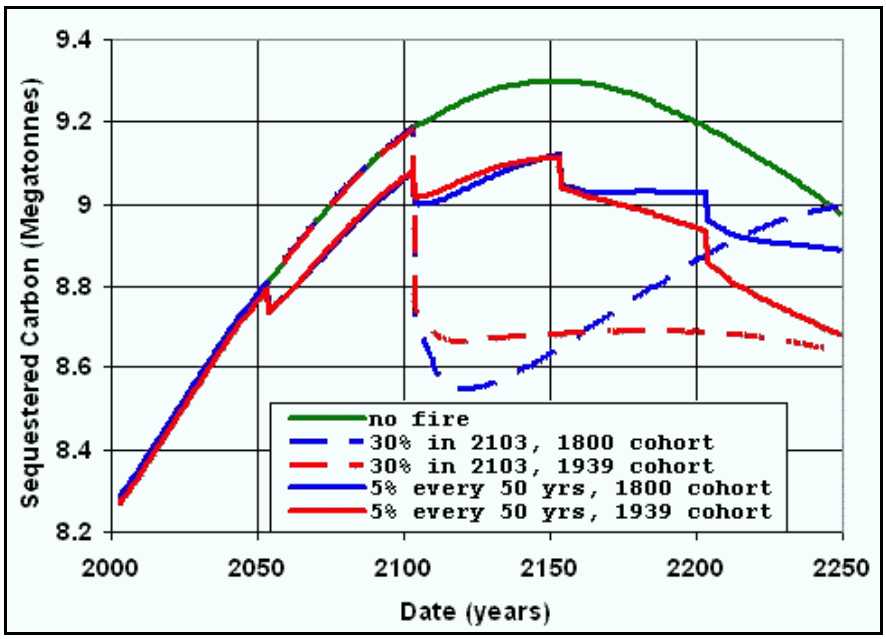

(a)

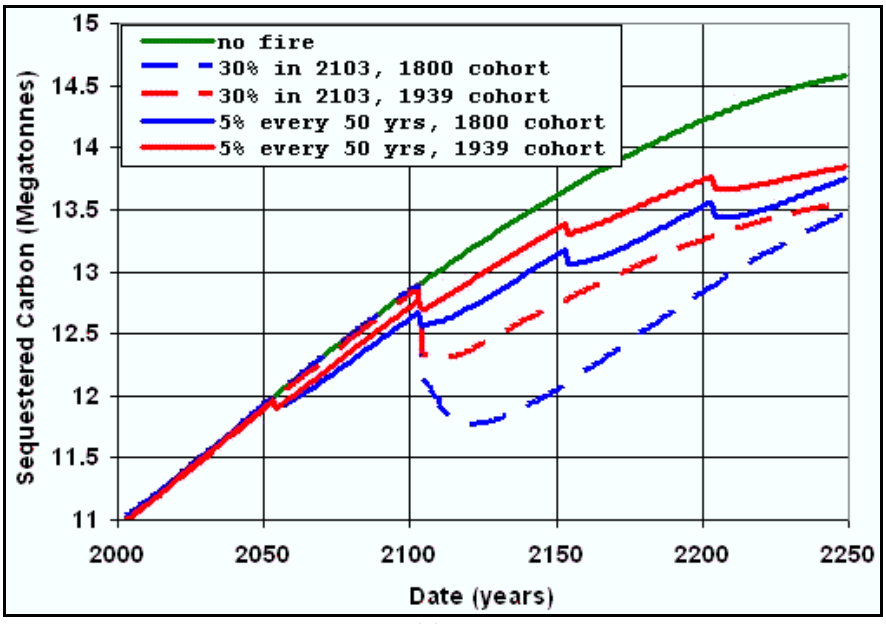

(b)

Figure 4. The effect of managed fire scenarios on the forecast, different stand ages, and different amounts of the catchment are burnt at different times. The green lines correspond to no fires. (a) low site index and low understorey biomass, (b) high site index and rainforest understorey biomass.

The uncertainty in understorey biomass is a major cause of the spread in the scenarios. For example the understorey biomass could be somewhere in between that observed in places such as 1. the Styx Valley in Tasmania with mature myrtles up to 2.3 m DBH (Figure 2.a), or near the Ada Tree in the Central Highlands, Victoria and 2. down to the scrubby type observed in some locations in the O'Shannessy catchment, Victoria (Figure 2.c). The lower-biomass understorey types are likely to be due to more frequent fires and poorer soils (Ashton, 1993) and snow damage (Ashton, 2000).

The impact of future fires on the forecast is worth considering and best explained with reference to the graphs of Figure 4. Two main fire possibilities were considered: 1. burning 30% of the catchment in one hundred years time from now, and 2. burning 5% of the catchment every 50 years. These two possibilities are further split into two: a) burning only the stands generated in 1800, and b) burning only the stands generated in 1939.

The uppermost line in Figure 4.a corresponds to a stand with a low site index and low understorey biomass (e.g. the forest in Figure 2.c). If a large amount of the oldgrowth (i.e. stands germinated in 1800) was burnt 100 years from now (and as many hectares were burnt as in the 1939 fires, i.e. 30% of the catchment) then there's a large carbon efflux (seen as a sudden, deep drop in the forecast) but after a further 150 years the sequestration has recovered and is the same as if no burning had occurred. A positive feature of this burn is that the trajectory, 250 years from now, has a positive slope, rather than the negative one it has in the absence of fire. A negative aspect of this burn is that the average carbon sequestered over the 250 years of the forecast period is 8.77 Mt-C whereas if there were no fires then the average carbon sequestered is 9.03 Mt-C. Burning the 1939 age cohort in place of burning the 1800 cohort produces less efflux, but the average carbon sequestered is lower at 8.72 Mt-C, as is the slope of the trajectory at 250 years from now, and the sequestered carbon at that date. If only 5% of the catchment is burnt at any one time and this is done every 50 years, then the trends are more moderate.

Considering the case where there's a high rainforest understorey biomass (and a higher average site index) as in Figure 4.b (e.g. for the forest in Figure 2.a), the results are simpler: all fires reduce both the average sequestration and the sequestration at 250 years from now and the trajectories are similar. However burning the oldgrowth does produce a marginally better trajectory 250 years from now.

The scenarios in Figure 4 assume that carefully managed fires are possible. However the spatial distribution of single-aged stands of different ages is varied, with patches of a single-age cohort stand as small as 250m^2, so it may not be physically possible to undertake burning of only one age cohort at a time. Consequently, in reality, the effect on carbon sequestration of any fire would be determined by the proportions of the different germination cohorts burnt and a graph of the results would be a combination of Figure 4.a and 4.b.

2.4 GIS raster output. The GIS raster format output allows examination of the spatial effects over time, for example the calculation of difference maps between different dates in the forecast, or even between different scenarios. A section of a difference map for the sequestration at years 2003 and 2160, for the O'Shannessy catchment is shown in Figure 5.

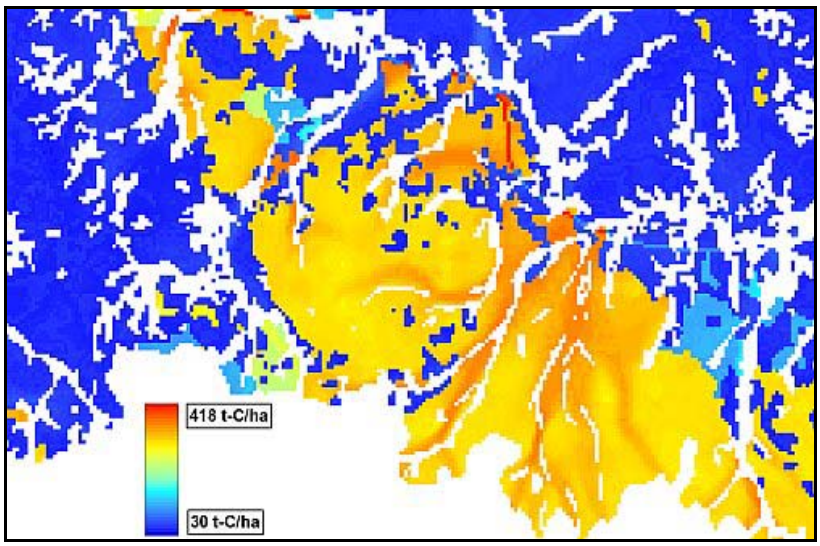

Figure 5. Difference map, between years 2003 and 2160, for the sequestration forecast of a portion of the O'Shannessy catchment.

The area shown in Figure 5 has a relatively low site index and understorey biomass, typical of that catchment. The large white area in the lower part of the Figure, is at higher elevation and contains *E. delegatensis*, which was not mapped in this study. The main contrast in the map is between the predominantly blue area and the predominantly orange area (or dark and light if viewing in grey scale); these correspond to the 1800 and 1939 germination cohorts respectively. However there is also contrast within the 1939 cohort, with the areas closer to rainforest gullies (the white elongated areas) having sequestered more carbon. Their higher sequestration is due to the relationship between site productivity and topographic wetness in the formula for stand height at age 50 years. This difference was calculated at only half way through the forecast and would be more pronounced after another 100 years with the 1800 cohort becoming a carbon source, due to the minimal understorey biomass for this scenario.

3 WITHIN-STAND VISUALISATION

Stem tapers (vertical profiles) were obtained either by direct measurement with a tape or by photography as described in Dean (2003). Cross-sections were obtained either by photography or measurement using tapes and a compass. Logged and unlogged buttresses were measured (Figure 6). Measurement was easier for unlogged buttresses due to large sizes of logging debris resting upslope on logged stumps. But after logging a unique and clearer view of buttress shape could be obtained for measurement by photography. The photographic data of horizontal cross-sections of felled trees was processed by the same image rectification process as for taper.

(a) **(b)**

Figure 6. (a) Lower portion of a photograph used to obtain longitudinal profile, O'Shannessy catchment, Victoria; showing tape and quadrat used in image rectification. (b) Photograph of a transverse section of logging debris, in coupe CO004E, Florentine Valley, Tasmania plus fluted outline (pink) and wrapped DBH tape (purple).

Measurement of cross-sections of standing trees was more complex: a tape was wrapped around at breast height (BH, 1.3 m) and all positions of spurs (convex parts of the undulating perimeter, the parts that are outermost and may extend to lateral roots) and flutes (concave parts of the undulating

perimeter) were recorded. For each spur in the buttress, three distances were measured: the tangent points to the tape and the most prominent point on the spur. For flutes the distance of the inner-most point and its perpendicular distance from the encircling tape were measured. A compass was used to record the direction of the tape between neighbouring spurs. The cross-sections were manually redrawn on paper and scanned to produce shapefiles (a GIS vector format) then a spline function was applied to smooth the data. Combining the vertical and horizontal profiles gives the 3D exterior volume of the stem but that combination process requires a model for the decrease in the depth of the flutes with increasing height up the stem. A "taper equation" can provide the exterior profile shape of the stem.

Five different taper equations (listed below) were tested: (1) the Kozak equation (Kozak, 1988); (2) a modified version of the Kozak equation where the exponent had less terms but still had flexibility; (3) the Bi equation (Bi, 2000) with its trigonometric functions; (4) the Nagashima & Kawata equation (abbreviated to Nag_Kaw) (Nagashima & Kawata, 1994; Nagashima *et al*., 1980) which has a separate term for the buttress region; and (5) a modified Nag_Kaw equation with a little more flexibility in the buttress region, obtained by adding an exponent to the height. The first term in equations (4) and (5) caters for the main "inner" part of the stem, which goes along its whole length, and the second term, which is exponential, caters for buttress flair. Equations (1) and (3) contain terms with direct reference to DBH and it is possible that such equations were not intended to be used with single tree taper curves (H. Bi, Sydney, 2003, personal communication; A. Goodwin, Hobart, 2003, personal communication) however all equations were treated equivalently in this part of the analysis and used only to fit a curved line to the data points rather than to represent the species in general. The number of parameters in each of the equations (1) to (5) was 9, 7, 7, 5 and 6, respectively.

$$d = a0 \times DBH^{a1} \times a2^{DBH} \times \left(\frac{1-\sqrt{ht/h}}{1-\sqrt{p}} \right)^{E1} \tag{1}$$

$$E1 = b1\left(\frac{ht}{h}\right)^2 + b2\log\left(\frac{ht}{h}+0.001\right) + b3\sqrt{\frac{ht}{h}} + b4\exp\left(\frac{ht}{h}\right) + b5\frac{DBH}{h}$$

$$d = a0 \times DBH^{a1} \times a2^{dbh} \times \left(\frac{1-\sqrt{ht/h}}{1-\sqrt{p}} \right)^{E1} \tag{2}$$

$$E1 = \exp\left(const + \left(\alpha \times \exp\left(\beta \times \frac{ht}{h} \right) \right) \right)$$

$$d = DBH \times \left(\frac{\log\sin\left(\pi ht/2H\right)}{\log\sin\left(\pi 1.3/2H\right)} \right)^{E12} \tag{3}$$

$$E12 = E1 + E2$$

$$E1 = a1 + a2\sin\left(\pi ht/2H\right) + a3\cos\left(\pi 3ht/2H\right) + \frac{a4H\sin\left(\pi ht/2H\right)}{ht}$$

$$E2 = a5DBH + a6\left(\frac{ht}{H}\right)\sqrt{DBH} + a7\left(\frac{ht}{\sqrt{H}}\right)$$

$$d = \left(Y \times \left(1 - \left(\frac{H - h}{H - ht} \right)^m \right) \right) + \left(\alpha \cdot \exp\left(-\beta \cdot ht \right) \right) \quad (4)$$

$$d = \left(Y \times \left(1 - \left(\frac{H - h}{H - ht} \right)^m \right) \right) + \left(\alpha \cdot \exp\left(-\left(\beta - c \right) \cdot ht^c \right) \right) \quad (5)$$

$$Y = 0.8851 DBH + 0.4184$$

$$H = 120\left(1 - \left(e^{-DBH^{3/2}} \right) 0.8851 DBH \right)$$

$$\alpha = 0.4066 DBH^{1.5197}$$

$$m = 0.8, \beta = 1.25, \; c = 0.95$$

In the above equations *d* is stem diameter, *ht* is height up the stem, *h* is tree height and *H* is maximum height of the species; *a0* to *a7*, *b1* to *b5*, *p*, *Y*, *H*, α, β, *m* and *c* were parameters that were refined by use of a genetic algorithm as described below to 22 *E. regnans* trees. Note that equations (4) and (5) are "two stage" equations. The rational number constants in the equations for *Y*, *H*, α, β, *m* and *c* (i.e. for equation (5)) were estimated from best fit curves to 22 *E. regnans* trees. During the fitting process for each taper curve, when using equations (1), (2) and (3), terms which were DBH dependent and height (ht) independent, were treated as constants and not refined; e.g. "DBH^{a1}" in equation (1). Thus the number of parameters was reduced for those equations: to 7, 5 and 6 respectively.

There were twenty two empirical individual-tree taper curves corresponding to DBHs ranging from 0.29 to 6.4 m, with an average of 190 points per curve. When using MS-Excel to fit the taper equations to the empirical taper curves we noticed that there could be a large range of parameter values that gave the same precision of fit, for any one curve and equation, depending on the starting values of those parameters before least squares estimation. Thus it was decided to use a "Genetic Algorithm" to calculate the best fit as it could scan a wide range of parameters and it was thus more likely to find the best minimum. The genetic algorithm works by selecting different populations of parameters then letting them evolve to fit the observations better (e.g. Michalewicz, 1992). This was followed by a simplex least-squares algorithm. The testing procedure was coded in Delphi, a language that can be described as a MS-Windows version of Pascal. The resultant best 30 fits for each empirical curve were selected. This process took about 60 hours per equation on a laptop with 500 Mb of RAM and running MS-Windows XP at 2GHz; with 100 populations evolving through 10,000 generations.

The goodness of fit of the different taper equations to the curves was tested using the root mean-squared error (RMSE) and by visual inspection of each curve. The plot of RMSE versus DBH showed that the error increased with tree size, which was expected. To compare the different equations, independent of tree size, we divided the RMSE for each equation for any one curve by the sum of the RMSEs, across all equations, to give a "relative RMSE" for that curve (Figure 7).

ISSN 1740-5955

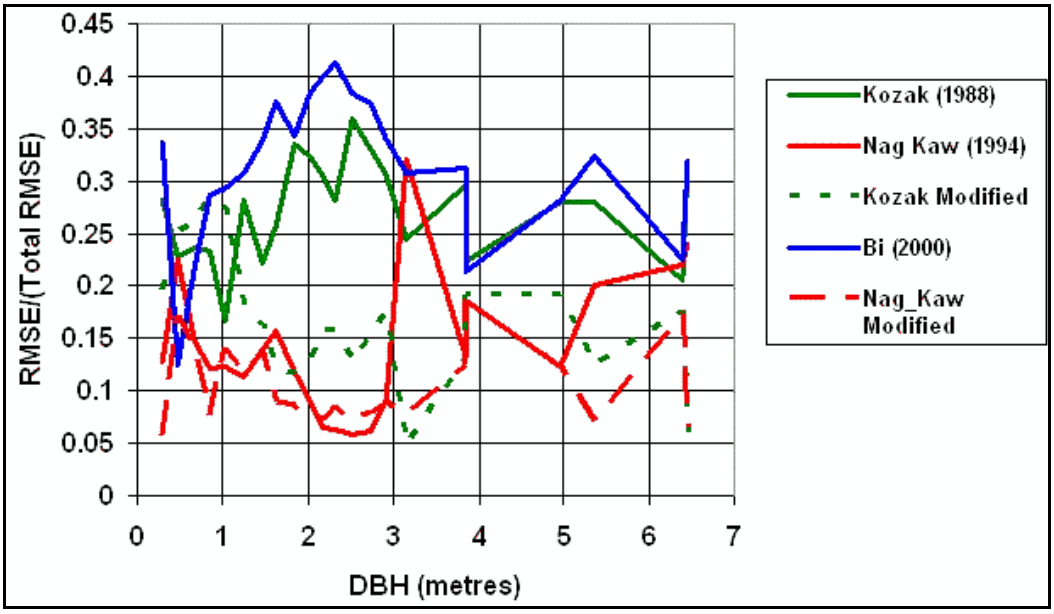

Figure 7. Taper fits for the five different taper equations, according to relative RMSE (RMSE divided by DBH) for the twenty two different curves.

The average relative RMSEs for the five equations were 0.27, 0.16, 0.30, 0.15 and 0.11 for equations (1) to (5) respectively. When comparing the goodness of fit for the different equations the general trends were that the Bi equation, (3), faired worst of all (except on the smallest trees), followed by the Kozak equation, (1). The modified equations, (2) and (5), did slightly better than the corresponding, original Kozak and Nag_Kaw equations. In general the Nag_Kaw pair faired better than the Kozak pair. These trends agreed with the impression gained from visual inspection.

In choosing which taper equation to use for volume calculation, we needed an equation with the following properties:

(i) it would fit individual trees reasonably well,
(ii) it had to account for the decreasing depth of flutes higher up the tree;
(iii) a physical interpretation of the parameters, to allow a discerning choice of parameter set,
(iv) it had to be defined at $ht = 0$ (ground level) for rendering purposes.

These criteria are perhaps more important in selecting a taper equation than the average Relative RMSE values. All of these criteria were met by the modified Nag_Kaw equation.

In the field of computer aided design (CAD), "extrusion" is the production of a 3D shape by applying a spatial translation to a planar section. With a simple assumption, the taper equation (5) can be used to "extrude" a tree's cross-section at BH to give the shape of a tree in 3D. The difference to the CAD-type extrusion is that the shape of the tree's cross-section must change as it is extruded. That change in shape is defined by the changing significance of the exponential term in equation (5) with height up the tree. Consider a point on the outside of a tree, somewhere on a typical cross-section at BH, neither out on the tip of a spur and not deep in a recess of a flute—then about a metre higher (or lower) up the stem—where is that chosen point with respect to the centre of the stem? At BH that point has a certain distance to the inner part of equation (5), it also has a certain distance out to the total equation (5), which includes the buttress flair term. If it is assumed that the ratio of those two distances above and below BH remains constant with height then the position of that point at any height up the stem (Figure 8.a) can readily be calculated. If one considers all the points on the cross-section at BH then applying this constant ratio concept, together with equation (5), gives the external shape of the tree, including fluting. In Figure 8.b the external shape was rendered using VRML.

ISSN 1740-5955

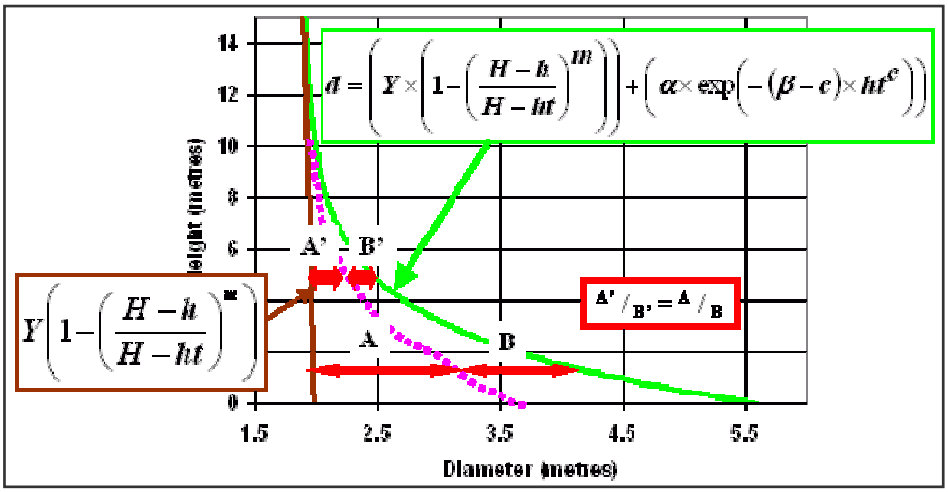

(a)

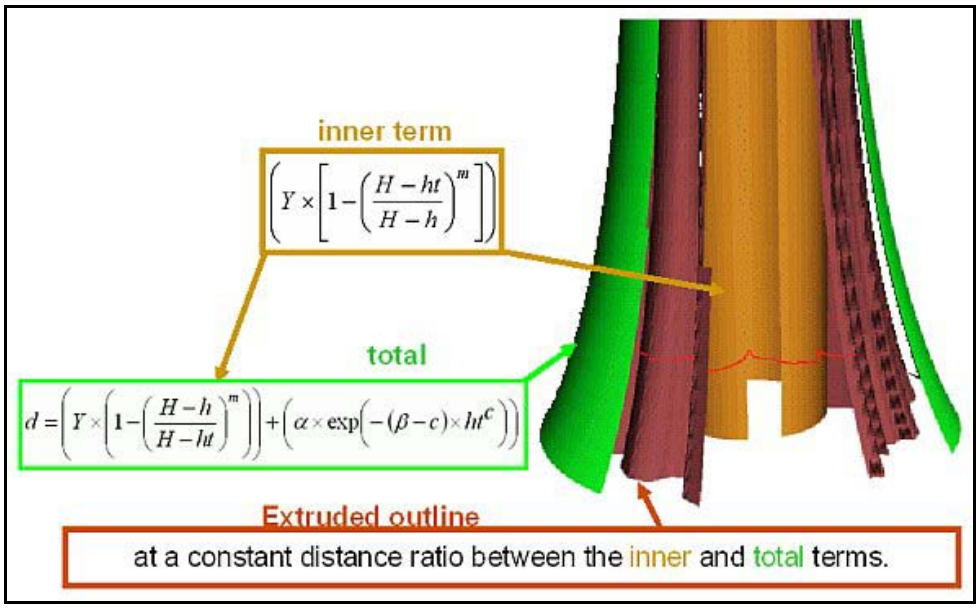

(b)

Figure 8. Calculated taper (using the modified Nag-Kaw equation, (5)) for a *E. regnans* with DBH 3.85 m, measured in Tasmania. (a) In 2D profile both the calculated taper with and without the buttress term are shown, plus the extrusion of a typical point on the cross-section at BH. (b) The cross-section (in red) is extruded to render a stem in 3D.

When that extrusion calculation is performed for each point on the cross-section the resulting set of points defines both the exterior shape of stem, and the stem volume. In the earlier version of CAR4D the inner part of the stem was approximated by a cone and the buttress region by an exponential term. This allowed volume calculations and rendering of the buttress region of trees in 3D but it was of relatively low precision. Also, without a suitable taper equation for oldgrowth trees, the stem above the buttress could not be drawn.

From empirical measurements and volume calculations, an equation was developed for stem volume as a function of DBH, which is one of the allometric equations in CAR4D. It has been revised by further fieldwork since its introduction in Dean *et al*. (2002a). The revised volume equation for *E. regnans* (using for 24 trees), using the fitted (5) taper model is:

$$V_{(5)} = 1100\left(1-\left(1+\left(\frac{DBH}{9.2}\right)^{2}\right)^{-1}\right) \quad R^2=0.95,\ RMSE = 34.2m^3 \qquad (6)$$

where $V_{(5)}$ is in m^3 and DBH is in metres. Nagashima *et al*., (1980) noted that the asymptotic value for H (equation (4)) is the maximum height for an individual tree (if the equation is fitted to one tree at a time). As we applied the modified equation, (5), to the *E. regnans* species as a whole then the asymptotic value of H is for that species. Our asymptotic value for H of 120 m corresponds well with early observations of *E. regnans*. As explained in Dean *et al*. (2003) the stands over 110 m tall no longer exist and reviews of reliably recorded heights of previously existing trees (e.g. Galbraith, 1937; and Hickey *et al*., 2000) suggest that our derived value of 120 m is quite reasonable as a maximum height.

Taper equations assume flat ground; therefore in order to draw trees on sloping and uneven ground the exterior of the stem had to be adjusted according to local micro-topography. Numerous oldgrowth trees were assessed on steep ground in Tasmania (WE008E, with an overstorey of *E. regnans* and *E. obliqua*). The topography is described in more detail above. Felled timber was moved by the logging contractors using predominantly cables and stationary winches (i.e. "cable logging").

Cross-sections (at 1.3 m) were recorded to see if the direction of spur development related to the aspect [of the slope]. No such relationship was found: some trees had spurs running down-slope (e.g. Figure 9.a to 9.c) and others had major spurs oriented perpendicular to the direction of slope and upslope but with none heading down-slope (e.g. Figure 9.d to 9.f). However, without destructive analysis it could not be determined if the old pith centres were still central within the mature buttress, and thus whether or not preferential growth had occurred in relation to aspect.

ISSN 1740-5955

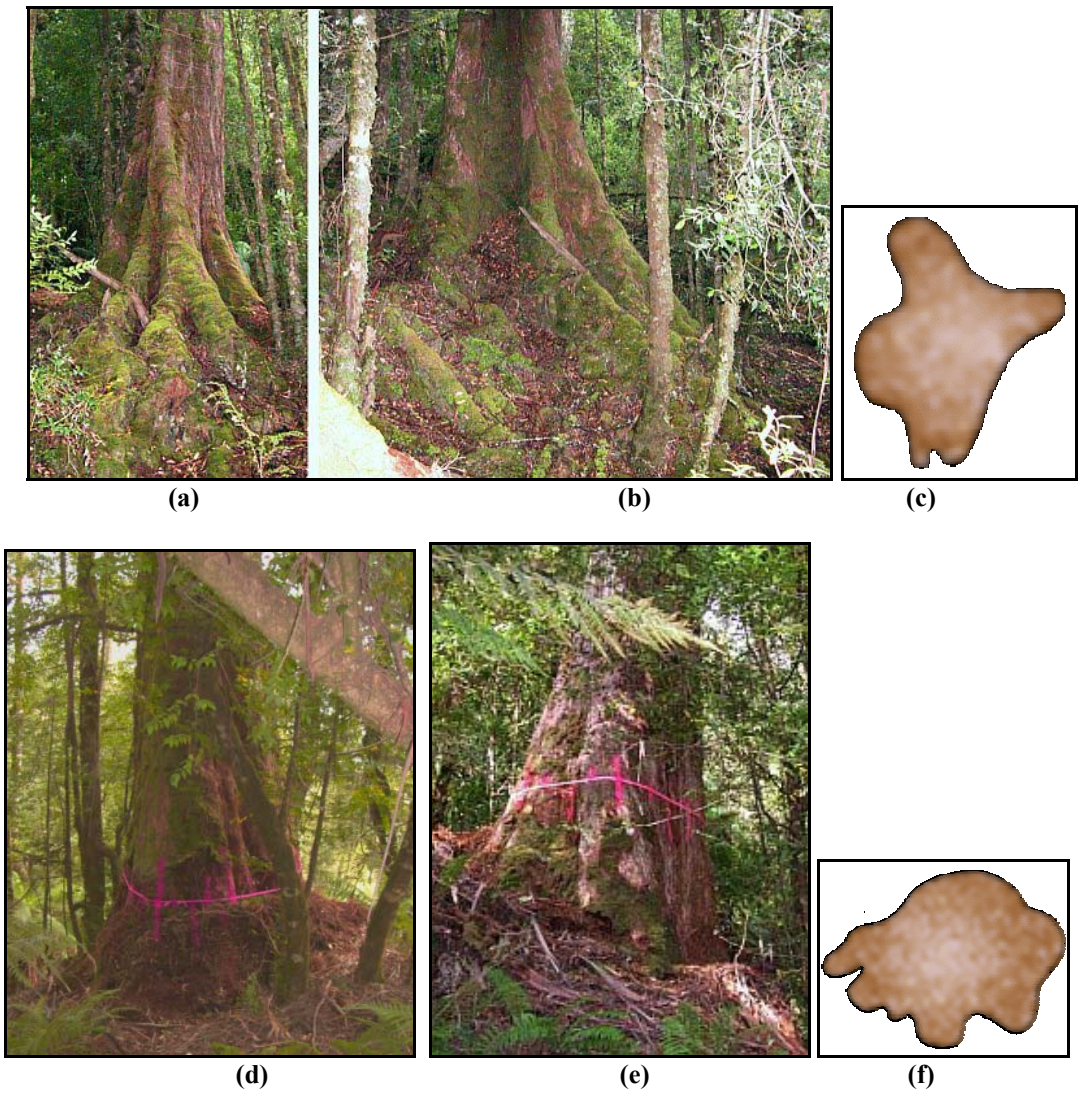

Figure 9. Profiles of the buttress region showing different arrangements of spurs for *E. obliqua* trees. The slope was 20º in coupe WE008E (Tasmania). In 9.b and 9.d the terrain slopes from left to right in the photograph. Tree-1 viewed from (a) down-slope and (b) the side, and Tree-2 viewed from (d) upslope and (e) the side. The diagrams of the cross-sections, (c) Tree-1 and (f) Tree-2, have the direction of down-slope going upwards on the page. Tree-1 has major spurs growing down-slope but Tree-2 has them growing upslope and to the side.

When rendering trees on slopes the localised adjustments to the taper equation used a series of trigonometric formulas. Each point on the exterior of the trunk (i.e. in a full 360º, whether spur or flute or somewhere in between) was adjusted individually, according to its height up the stem, and according to the slope of the ground between it and the centre of the tree. Points on the tree closer to the ground were adjusted more. To differentiate the scale over which slope of land may be measured and to specify a unique direction, we use the term "micro-slope" for the slope of the ground at a small scale—from the centre of the tree out towards each perimeter point on the tree's cross-section.

For each perimeter point, at each height up the tree, the micro-slope was calculated by projecting the point vertically, and comparing where that line intersected the ground, with the level of the ground at the centre of the tree. The amount of vertical adjustment for each perimeter point depended on both its distance from the ground (before projection) and on its relative height up the tree. Points were moved vertically by a fractional height adjustment (*fha*), which was greater in the buttress region:

$$fha = \exp\left(-30 \times \left(h / ht\right)\right) \tag{7}$$

where h and ht are as given in (5).

There was little information available on the width of a buttress as a function of slope, therefore the radial adjustment was subjective but it was calculated according to what should intuitively provide both stability and a realistic appearance. The relative adjustment to the radius as a function of micro-slope is fra:

$$fra = fsa / \sin(45°) \tag{8}$$

where fra is the fractional adjustment to the radius, and fsa is 0.35 for an up-micro-slope and 0.75 for a down-micro-slope. The value of sine45º was used as it gives a change of 25%, which was seen to approximate the observations most closely. The adjustment to the radius, ra, is a function of both relative height and micro-slope:

$$ra = fha \cdot fra \cdot \left|\sin(s)\right| \tag{9}$$

where s is the angle of micro-slope (positive for an up-micro-slope). The adjusted x and y coordinates of a perimeter point with pre-adjusted coordinates [x_old, y_old], relative to the centre of the tree are x_new and y_new given by:

$$x\_new = x\_old + x\_ol \cdot ra \ , \ y\_new = y\_old + y\_old \cdot ra \tag{10}$$

and the new height of the perimeter point is h_new, given by:

$$h\_new = h + fha \cdot \left(h\_ground_{[x\_new, y\_new]} - h\_centre\right) \tag{11}$$

where $h\_ground_{[x\_new, y\_new]}$ is the height of the ground at [x_new, y_new], and h_centre is the height of the centre of the base of the tree, i.e. the ground elevation at which the original seed grew. Spiral grain, which occurs in many individual *E. regnans*, was included by rotating the cross-section at each height step before adjusting for micro-slope.

The above equations and concepts are coded in a C++ program which also writes Javascript and VRML output. An example of adjustments for various localised terrain variability is displayed in Figure 10 as a VRML world. The number of trees in any given year and their diameters at 1.3 m were calculated using CAR4D. However, for demonstration purposes, the cross-sections of real trees measured in the field were used. Their individually estimated taper parameters (for equation (5)) were used to render the solid VRML model for each tree.

Although the 2D location of trees could in principle be simulated from a spatial ecological model, a random number generator was used in the present work to locate the trees over one quarter hectare square. The output format was VRML 2.0, displayed in Netscape 4.77, Microsoft Internet Explorer or in Socket45 using the plugin CosmoPlayer.

The ground surface was created by scaling a 50 m × 50 m digital elevation model of a mountain range by 1/250 horizontally and 1/35 vertically. Ground colour was assigned according to calculated topographic wetness. Both elevation and wetness data were in ESRI's ASCII grid format.

Figure 10. A stand-level VRML world output showing adjustment to the taper for various terrain. Note that spiral grain is easily included in the tree models, as is change in colour corresponding to the thicker bark in the buttress region and the lighter, thinner bark higher up.

The VRML world shown in Figure 10 does not change with tree age, i.e. it is not a dynamic animation. For animation the spurs in the buttress must be seen to grow. For stability, the prominence of spurs in the buttress region increases as trees mature (Ashton, 1975; Nicol & Ray, 1996), but then decreases for mechanically stable, mature trees with more radially-even growth (e.g. Julin & Farr, 1989). This increase then decrease in cross-sectional area-deficit was modelled and reported in Dean *et al*. (2003) and the maximum cross-sectional area deficit (of ~40%) was found to be when the DBH was 3.34 m. That equation was used in the present work to model spur development as a function of age. Spurs were modelled as functions of (a) an angle from north, (b) relative prominence, (c) angular influence or spread, and (d) age. In reality their growth is also dependent on specific, localised environmental stresses that occur at different times in the life of the tree, but in this preliminary model all spur growth was set to occur simultaneously. Also spur growth need not be predominantly away from the centre, especially so for secondary spurs growing off larger ones, but that complexity was not modelled here either. Similarly, the bifurcation of spurs into smaller lateral roots, more prominent as they reach down-slope, was not modelled.

The angle from north was set arbitrarily (for demonstration purposes), as was the relative prominence and the angular influence. The angular influence of each spur was parameterised as a ("logistic") function of angle away from the centre of each spur:

$$Influence = \frac{1}{1 + n.e^{k^{-1}(1-|\cos\theta|)}} \tag{12}$$

where n = 0.005 and k ranges from 0.005 to 0.02. The influence of each spur then ranges between 0 and 1 as shown in Figure 11. Although the top of the curves in Figure 11 appear flat the shape of the spur will still be rounded, with a radius equal to its distance from the tree centre. Different spurs around the tree are assigned different relative sizes (e.g. from 0.5 to 1) and for each point around the cross-section that relative size is multiplied by the value of influence in equation (12) to give an adjustment to its radius from the centre of the tree.

ISSN 1740-5955

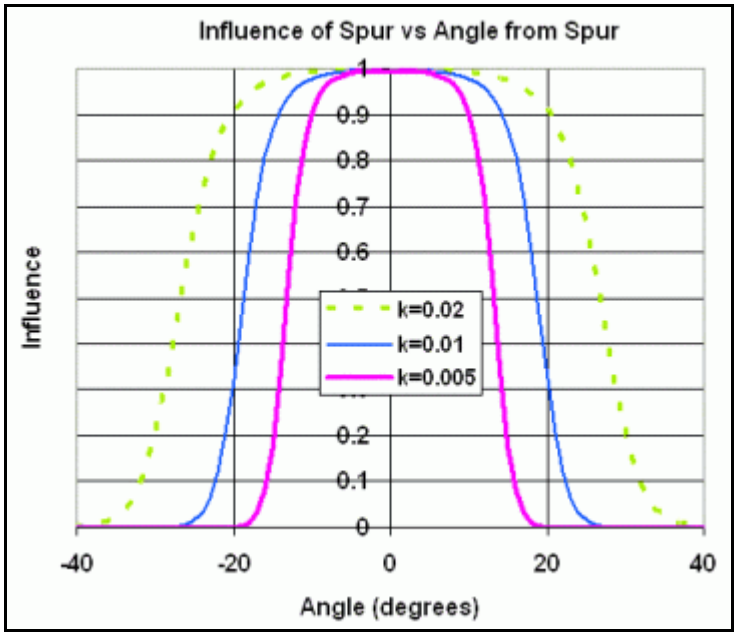

Figure 11. The varying angular influence of a spur from (7).

A VRML model for a tree corresponding to this type of buttress development is shown in Figure 12. The viewing of the animation is controlled by Javascript written to the .WRL file by the C++ program. The Javascript and its onscreen interface follows that of Bell *et al*. (2000). Stepping through the animation is controlled on screen within the VRML world and allows fly-throughs while the animation is stepping through time. For an animated GIF format rendition of the tree growth shown in Figure 12 please either contact the author or it may be found on the profile models section of the FMA.

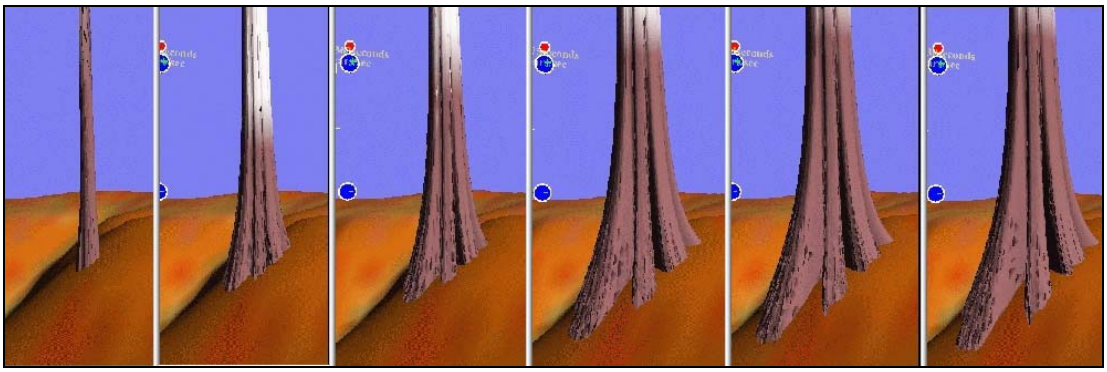

Figure 12. Frames from a VRML animation of stem growth for a single tree with a buttress containing seven spurs. Ages from left to right are 50, 100, 150,250, 350 and 450 years with DBHs of 0.57, 1.22, 1.58, 2.32, 2.85 and 3.23 m respectively. The number of spurs was seven, with angles from north of 10°, 75°, 105°, 155°, 225°, 275° and 315°; relative influences of 0.7, 0.74, 0.95, 0.88, 1, 0.5 and 1; and values for k (in equation (12)) of 0.01, 0.02, 0.05, 0.02, 0.01, 0.005 and 0.01 respectively.

4 DISCUSSION & CONCLUSIONS

The process flow in CAR4D is suited to a variety of scenario tests including comparison of management options, comparison of the influences of parameter settings, and suitable for a variety of output styles each with their own specific uses. It is hoped that implementation of the model on web servers will happen in the not to distant future along with the capability to cater for *E. obliqua* and acquisition of more data on the understorey biomass, which can be a major component of the total forest biomass in higher site quality locations. The balance between sequestration and efflux is both a

spatial and long-term concern and further usage of CAR4D should yield results pertinent to current greenhouse gas budget decisions in Australia. Results from the unit area analyses showed that: a) wood products are a minor carbon pool relative to the carbon sequestered in a mature forest; b) the conversion of oldgrowth to plantation (or "regen") is accompanied by a large carbon efflux in the long term, if the harvesting cycle length is less than about 300 yrs; c) plantation as afforestation of previously cleared agricultural land is most likely viable; and d) the optimum cycle length for wood products pool is about 50 yrs for *E. regnans* but the optimum cycle length when considering all carbon pools is about 400 yrs. The duration of 50 yrs is also equal to the optimum year for the average annual stem volume increment and for the minimal water output from the stand.

Catchment level forecasts revealed that more information is needed about several aspects before a reasonably precise forecast can be given. These include: a) understorey biomass, b) mean catchment level site index, c) whether or not competition forces self-thinning to continue beyond 200 yrs, d) proposed fire management or naturally precipitated fires, e) previous fire history, and f) influence of site-index-independent potential growth. For fire management it was shown that it is not just the differences in sequestration at 250 years time from now that could be of concern, but also the trajectory at that time and the average amount of carbon sequestered over the forecast period. The *E. regnans* forests of the O'shannessy catchment in the Victorian Central Highlands have a relatively low understorey biomass (compared with those in the Styx Valley or the Ada tree localities) and hence a net carbon efflux is forecast upon senescence. However, the forecast does not imply that anthropogenically induced fires are necessary to prevent a carbon efflux. Other possible options are: (i) fires started from lightning strikes are inevitable over the forecast period of 250 yrs; (ii) increase in fires accompanying increases in human population (Venevsky *et al*., 2002), and (iii) intentional, lateral shifts of the dirt roads in the catchment, every 50 yrs (the felled trees could be used for lumber and the old road surfaces could be afforested with *E. regnans* saplings or successional rainforest species from local seed stock).

As a corollary to adjustment of the stem for sloping ground it is noteworthy that the standard practice in forest mensuration is to measure DBH from the high side of a tree. However, for a tree that is on a slope this ground position will keep getting higher as the tree grows. This in turn means that the measured DBH, in successive years for example, isn't measuring the increase in the radial growth of the tree, instead the recorded increments in DBH will be smaller as they are being made higher up the tree. (E.g. using the modified Nag_Kaw equation it was found that for a tree of DBH 3.5 m, on a 25° slope, the DBH is being measured at 1.8 m rather than at 1.3 m). There are several obvious implications of this for DBH and taper curves measured on sloping ground for mature trees. For example, a tree on a slope will appear slimmer near ground level than it really is, and of lesser volume; or stated from a different viewpoint: large, mature trees on flat ground will appear to have a buttress wider than normal.

Other obvious possible improvements include modelling: the understorey, which can be a major component of the biomass; the decay processes including trunk hollows; and for loftier views, the branches and foliage.

Although fly-throughs are possible in the VRML output the content of the output is still under development with planned improvements including: a) animation between years of, for example, self-thinning, stem growth, senescence and carbon fluxes, b) inclusion of understorey, which can be a major component of biomass. d) inclusion of branches, e) bifurcation of spurs into smaller lateral roots, and f) biologically realistic positions for the trees.

CAR4D has shown to be versatile and useful both for management and for development of the science related to carbon sequestration in forests. Visualisation is already being used to show ecological influences on tree growth for single trees and in ecosystem visualisation (Prusinkeiwicz *et al*., 2001). Potential uses of the VRML format output are: a) aid for comparison of different carbon sequestration models, b) visualisation of carbon dynamics as a teaching aid (e.g. showing falling trees and decay CWD), c) an aid to forestry or ecology management, d) insight into the influence of ground slope on forest mensuration, and e) ray tracing using the 3D data itself could provide input to NPP based carbon models.

5 ACKNOWLEDGEMENTS

The authors would like to thank Bevan McBeth, Leigh Edwards and Leandra Bennett for assistance with field work; Forestry Tasmania and Parks Victoria for access to forests, Yoav Daniel Bar-ness, Mick Brown, Adrian Goodwin and John Hickey for helpful discussions; Brendan Mackey for

instigating the initial project and for helpful discussions; and the CRC for Greenhouse Accounting for funding.

6 REFERENCES

Ashton, D.H. (1975) The Root and Shoot Development of Eucalyptus regnans F. Muell. *Australian Journal of Botany*, 23, 867-87.

Ashton, D.H. (1993) Fire in tall open-forests (wet schlerophyl forests). In: Gill, A.M., Groves, R.H. and Noble. I.R. (eds.) *Fire and the Australian Biota*, Australian Academy of Science, Canberra, pp339-366.

Ashton, D.H. (2000) The Big Ash forest, Wallaby Creek, Victoria —changes during one lifetime. *Australian Journal of Botany*, 48, 1-26.

Barnard, S. (2000) Information:- The Making Of Tarzan–The Deep Canvas Process. http://www.dvdweb.co.uk/new/news.asp?mainID=366 Viewed on 02-04-2004.

Bassett, O.D., Edwards, L.G. and Plumpton, B.S. (2000) A comparison of four-year-old regeneration following six silvicultural treatments in a wet eucalypt forest in southern Tasmania. *Tasforests*, 12, 35-54.

Bell, M., Dean, C. and Blake, M. (2000) Forecasting the pattern of urban growth with PUP: a web-based model interface with GIS and 3D animation. *Computers, Environment and Urban Systems*, 24, 559-581.

Bi, H. (2000) Trigonometric variable-form taper equations for Australian eucalypts. *Forest Science*, 46(3), 397-409.

Bishop, I.D., Fasken, G., Ford, R., Hickey, J., Loiterton, D., Williams, K. (2003) Visual simulation of forest regrowth under different harvest options. In Buhmann, E. and Ervin, S.M. (eds.) Trends in Landscape Modelling, Proceedings at Anhalt University of Applied Sciences, Dessau, Germany, 15-16th May 2003. Herbet Wichmann Verlag, Heidelberg, pp. 46-55.

Cochrane, G.R. (1969) Ecological Valence of Mountain Ash (*Eucalyptus regnans* F. Muell.) as a key to its distribution. *The Victorian Naturalist*, 86, 6-10.

CMLabs (circa 2003) Seeing the Forest Through the Trees. Training simulator for the logging industry made possible with Vortex physics. http://www.cm-labs.com/customers/Oryx/ Viewed on 02-April-2004.

Dean, C. (2003) Calculation of Wood Volume and Stem Taper Using Terrestrial Single-Image Close-Range Photogrammetry and Contemporary Software Tools. *Silva Fennica,* 37(3), 359-380.

Dean, C., Roxburgh, S. and Mackey, B.G. (2003) Growth Modelling of *Eucalyptus regnans* for Carbon Accounting at the Landscape Scale. In: Amaro, A., Reed D and Soares, P. (eds.) *Modelling Forest Systems*, CAB International, Wallingford, UK, pp. 27-39+plates.

Dean, C., Roxburgh, S. and Mackey, B.G. (2004) Forecasting Landscape-level Carbon Sequestration using Gridded, Spatially Adjusted Tree Growth. *Forest Ecology and Management,* 194(1), 109-129.

Dzierzon, H., Sievänen, R., Kurth, W., Perttunen, J., Sloboda, B. (2003) Enhanced Possibilities for Analyzing Tree Structure as Provided by an Interface between Different Modelling Systems. Silva Fennica, 37(1), 31-44.

Ervin, S. M., and Hasbrouck, H.H. (2001) *Landscape Modelling: digital techniques for landscape visualisation*. McGraw Hill, New York, 290pp.

Galbraith, A.V. (1937) *Mountain Ash (Eucalyptus regnans -F.von Mueller) A general treatise on its silviculture, management, and utilization*. H.J. Green, Government Printer, Melbourne, 51pp.

Gigliotti, C. (2002) Reverie, Osmose and Ephémère. *n.paradoxa*. 9, 64-73.

Gilbert, J.M. (1958) Eucalypt–rainforest relationships and the regeneration of the eucalypts. PhD thesis, University of Tasmania, Hobart, Australia.

Grierson, P.F., Polglaise, P.J., Attiwill, P.M., and Adams, M.A. (1993) *Carbon Storage in Victoria's Forests.* In Shelley Burgin (ed.) *Climate Change*, *Occasional papers in biological Sciences*; no. 1. University of Western Sydney, Hawkesbury, NSW, Australia. pp81-99. ISBN 1863410813.

Hickey, J.E., Kostoglou, p., and Sargeson, G.J. (2000) Tasmania's tallest trees. *Tasforests*, 12,105-121.

Julin K.R., Farr W.A. (1989) Stem Fluting of Western Hemlock in Southeast Alaska. U.S. Dept. of Agriculture, Forest Service, Portland Northwest Research Station, Portland, Oregon. 8pp.

Kozak, A. (1988) A variable-exponent taper equation. *Canadian Journal of Forest Research*. 18, 1363-1368.

Kostoglou, P. (2000) A survey of ultra tall eucalypts in southern Tasmania, A report to Forestry Tasmania, Hobart, Australia.

Liski, J., Pussinen, A., Pingoud, K., Makipaa, R. and Karjalainen, T. (2001) Which rotation length is favourable to carbon sequestration? *Canadian Journal of Forest Research*, 31, 2004-2013.

Knauft, F.-J. (2004) Landscape visualization with forest growth. 4th International Workshop on Functional-Structural Plant Models, 7-11th June, 2004, Montpellier, France.

Keith, H., Barrett, D. and Keenan, R. (2000). Review of allometric relationships for estimating woody biomass for NSW, the ACT, Vic, Tas and SA. *NCAS Technical Report 5b*, Australian Greenhouse Office, Canberra.

Michalewicz, Z. (1992) Genetic algorithms + data structures = evolution programs. Springer-Verlag, Berlin, 387pp.

Nagashima, I., and Kawata, N. (1994) A stem taper model including butt swell. *Journal of the Japanese Forestry Society*, 76(4), 291-297.

Nagashima, I., Yamamoto, M., and Sweda, T. (1980) A theoretical stem taper curve. *Journal of the Japanese Forestry Society*, 62(6), 217-226.

Nicol B.C., Ray D. (1996) Adaptive growth of tree root systems in response to wind action and site condition. Tree Physiology, 16, 891-898.

Prusinkeiwicz, P, Mündermann, L., Karwowski, R., Lane, B. (2001) The use of positional information in the modelling of plants. ACM SIGGRAPH, Los Angeles, California, 12-17th August, 2001, p289-300.

Szijártó, G., Koloszár J. (2003) Hardware Accelerated Rendering of Foliage for Real-time Applications. Spring Conference on Computer Graphics, 24th-26th April 2003, Budmerice, Slovakia.

Van Pelt, R., Sillet, S., and Nadkarni, N.M. (2004) Quantifying and Visualizing Canopy Structure in Tall Forests; Methods and a Case Study. In Lowman, M.D. and Rinker, H.B. (eds.) Forest Canopies, Elsevier Academic Press, San Diego, CA. pp. 49-72.

Venevsky, S., Thonicke, K., Sitch, S. and Cramer, W. (2002) Simulating fire regimes in human-induced ecosystems: Iberian Peninsula case study. *Global Change Biology,* 8, 984-998.

Vertessy, R.A., Watson, F.G.R., O'Sullivan, S.K. (2001) Factors determining relations between stand age and catchment water balance in mountain ash forests. *Forest Ecology and Management*, 143(1-3), 13-26.